Analytical Study on the Effect of Geometry of Umbrella Anchors in Clays

Shutao Zhang[1,2], Jun Peng[2], Yong Dai[3], Hongyang Huang[4,*], Tingting Li[4]

[1]State Key Laboratory of Hydraulic Engineering Intelligent Construction and Operation, Tianjin University, Tianjin, 300350, China
[2]CAAC Central & Southern Airport Design & Research Institute (Guangzhou) Co., Ltd., Guangzhou, 510405, China
[3]Zhonghai Construction Co., Ltd, Guangzhou, 510000, China
[4]Changjiang River Scientific Research Institute, Wuhan, 430014, China

*Corresponding author's e-mail:273746@whut.edu.cn

Abstract. Umbrella anchor has large anchoring force and high timeliness, which is an effective technical measure for rapid reinforcement of soil engineering. However, the influence of anchor plate geometry on its anchoring characteristics is not clear. Therefore, indoor pull-out model tests of rectangular anchor plates with different geometric sizes were carried out, and the variation law of pull-out load with displacement in 95 % compacted clay was tested. The influence of anchor plate geometric size on anchorage characteristics was calculated and analyzed by Plaxis finite element software. The results show that the bearing capacity experiences the compaction growth stage, the shear failure growth stage and the shear residual attenuation stage with the increase of displacement. The maximum bearing capacity increases with the increase of anchor plate area, but the bearing capacity per unit area decreases with the increase of area, and the larger the buried depth, the greater the attenuation. During the uplift process, the soil around the anchor plate shows a gradual failure process, and the fracture surface continues to extend until it penetrates. Under the condition of shallow burial (buried depth ratio = 2), the fracture surface is generated from the outer edge of the upper part of the plate, and develops upwards and outwards until the soil surface.Under the condition of deep burial (buried depth ratio = 8), the fracture surface develops directly above the plate, forming an annular fracture surface inside the soil. The change of the length-width ratio of the anchor plate changes the development process of progressive failure. With the increase of the long side of the anchor plate with the same width, the failure form of the soil around the anchor at the same buried depth is more shallow. This phenomenon makes the bearing capacity of the anchor plate per unit area decrease with the increase of the area. The research results are reliable, which provides theoretical support for the further popularization and application of umbrella anchor.

Keywords: umbrella anchor; clay; geometric size; anchoring characteristics; progressive failure.

P. Xiang et al. (eds.), *Proceedings of the 2023 5th International Conference on Hydraulic, Civil and Construction Engineering (HCCE 2023)*, Atlantis Highlights in Engineering 26,
https://doi.org/10.2991/978-94-6463-398-6_38

1 Introduction

In complex geologic slope engineering problems, such as expansive soil slopes, higher load-bearing and deformation-resistant requirements are put forward for anchoring and supporting structures. In order to solve this engineering problem, the Yangtze Academy of Sciences developed a new type of umbrella anchor structure and supporting rapid reinforcement technology based on the characteristics of the end expanding anchors, which was applied to the South-to-North Water Diversion Central Line canal slope rescue, and achieved excellent results[1~2]. However, the analysis of the anchoring mechanism of umbrella anchor structure is not sufficient in the current study, which affects the further promotion of umbrella anchor anchoring technology.

In view of the structural characteristics of umbrella anchor, the umbrella anchor is regarded as an expanded anchor with a very thin length of the expanded section, so that the research object can be simplified to the anchor plate model, and the research and analysis can be carried out in this way. Regarding the research on anchor plate pullout bearing problem, at present, there are mainly field and indoor model test, limit equilibrium analysis, limit analysis and finite element and other numerical methods[3~6]. It has been shown[7~10] that the upward pullout bearing process of anchor plate in clay soil is closely related to factors such as soil strength, depth of burial, and inclination angle of the anchor plate, but the influence of the geometry of the anchor plate has rarely been analyzed.

Yu Long et al[8] used elastic-plastic finite element method to analyze the uplift bearing process of bar-shaped anchor plate in normal consolidation clay, analyzed the influence of burial depth ratio, inclination angle and anchor soil bond form on the uplift bearing of anchor plate, and did not elaborate the influence of anchor plate geometry; Wang Lizhong[9], Yu Shengbing[10], etc. based on the upper limit theory of limit analysis, solved the upper limit solution of the uplift bearing capacity of the bar-shaped anchor plate, but the process also only considered the burial depth and the inclination angle. However, only the effects of the embedment ratio and the inclination angle of the anchor plate on the pullout bearing capacity and damage surface characteristics of the anchor plate were considered in the process.

On the one hand, in some sandy soil anchor plate pullout resistance research, scholars have observed the effect of anchor plate geometry on pullout capacity, and some scholars have also discussed this issue in depth. Hao Dongxue et al[11] studied the effect of anchor plate type and size on the bearing characteristics during the upward pulling process of anchor plate based on the small scale pullout model test of anchor plate with different geometries. The study shows that the spiral anchor and flat anchor plate have the same load bearing characteristics under the same burial depth ratio and diameter conditions. At the same burial depth ratio, the load carrying capacity coefficient of 50mm diameter anchor plate is smaller than that of 20mm diameter anchor plate, but its destructive displacement ratio (the ratio of the displacement corresponding to the ultimate uplift force to the diameter of the anchor plate) is higher; Chen Rong et al.[12] analyzed the dimensional effect of the uplift bearing of a circular anchor plate in dense sand by means of model test and finite unit method. It was found that the coefficient of upward pullout bearing decreases with the increase of anchor plate diameter, and this

phenomenon is more significant under the condition of increasing burial depth ratio. Meanwhile, Chen Rong attributed the size effect of anchor plate to two reasons. On the one hand, it is caused by the change of soil strength due to the change of stress level in the pulling process, and on the other hand, it is caused by the asymptotic damage in the pulling process; Shi Danda et al[13] analyzed and investigated the deformation characteristics of the soil around the anchors during the pulling process by combining with the DIC (Digital Image Correlation Technique) technology in the process of indoor pulling model test. The study shows that, under the same burial depth ratio, with the increase of diameter, the ultimate bearing capacity of the anchor plate pullout and the damage displacement to reach the ultimate bearing capacity increase significantly, but the pullout bearing capacity coefficient Ny decreases, and the change of the diameter has less influence on the shape of the displacement influence zone of the soil around the anchor.

On the other hand, in some earlier studies on the pullout bearing capacity of anchor plates in saturated clay, scholars have noted that the geometry of the anchor plate will have an effect on the anchor plate bearing capacity, but further analysis is not sufficient.Das et al.[14] carried out indoor circular and rectangular anchor plate modeling experiments to investigate the pullout bearing characteristics of the anchor plate foundations with different depths of burial under the conditions of the aspect ratios from 1 to 5. It was shown that, under the given soil conditions, with the increase of the anchor plate foundation aspect ratio, the anchor plate critical burial depth ratio H/B (the burial depth dividing shallow and deep burial is the critical burial depth, and the critical burial depth ratio is the ratio of the critical burial depth to the characteristic width of the anchors) will increase, and when the aspect ratio L/B>4, the critical burial depth ratio of the rectangular anchor plate foundation is about 1.6 times of that of the square anchor plate foundation; Rowe&Davids[15]. Based on the model test and small deformation finite element analysis method, the rectangular anchor plate and strip anchor plate with the length-to-width ratio of 3-8 are analyzed for the pullout bearing characteristics, and the study shows that the anchorage capacity per unit area of the anchor plate will be improved by the reduction of the length-to-width ratio. In practical applications, the pullout bearing capacity of rectangular anchor plate with aspect ratio L/B>5 (corresponding to 5 and 8 rectangular anchor plates in the article) is similar to that of strip anchor plate; Wang et al[16] studied the pullout bearing capacity of anchor plate based on the finite element analysis method, and the results showed that, for the case where the anchor soil is always cohesive, the rectangular anchor plate with aspect ratio L/B>6 can be regarded as a strip anchor plate; without considering the soil body Under the condition of self-weight, the bearing capacity coefficient of a circular anchor plate with a given diameter will be slightly larger than that of a square anchor plate with the same width, and the critical embedment ratio of a rectangular anchor plate increases with the increase of the aspect ratio.

From the results of the above analysis, it can be seen that the anchor plate anchorage bearing characteristics in clay soil is affected by the geometry, but lack of further analysis of the internal causes, based on this, this paper in the indoor model test based on the use of Plaxis series finite element analysis software, based on the hardened soil model (HS model) on the rectangular anchor plate uplift process simulation, so as to

reveal the umbrella anchor uplift geometry in the clay soil to pull up the bearings. The reason for the influence of the uplift geometry of umbrella anchor in clay soil is revealed.

2 Drawing model test

2.1 Test Program

Different sizes of rectangular anchor plate pullout model tests were carried out at different burial depths to analyze and study the influence of the geometry of the anchor plate. The test program is shown in Table 1.

Table 1. Test plan

working condition	Height(cm)	burial depth ratio *H*/*B*	aspect ratio *L*/*B*
1	10	2	1.4
2	10	4	1.4
3	10	6	1.4
4	10	8	1.4

The inner diameter of the model box used in the test is 80*80*100cm, one side of the acrylic board, the board is painted with a coordinate grid, in order to observe and analyze the deformation of the soil body in the process of pulling the development of morphology. Test anchor plate for one side with a smooth ball steel plate, thickness 1cm, ball side for contact with the acrylic plate to reduce the impact of plate friction on the test. The test anchor bar is a 1cm diameter steel bar, which is connected to the anchor plate by threaded bolts.

2.2 Clay Characterization and Sampling

The test soil samples were taken from Nanyang, Henan Province, which belongs to high liquid limit clay. The physical properties of the soil samples measured in the indoor tests are shown in Table 2. Before the tests, the wet soil samples were firstly configured according to the optimal moisture content, and then the soil layers were filled. The soil layer was filled in layers with a height of 5cm, and the surface of each layer was scraped to increase the bonding between layers. During the filling process, the thickness of the soil layer attached to the anchor plate was set at 10cm, and when the soil was filled to the depth of the anchor plate, the anchor plate was placed flat on the surface of the soil layer, and the anchors were kept vertical by pulling a line to locate the anchors, and at the same time, clamps were set on the top of the model box to fix the position of the anchors, so as to prevent the anchors from tipping over during the subsequent filling and compacting process. After making samples, the weight and volume of soil samples were measured to calculate the actual degree of compaction, and the compaction degree of all soil layers in this test was about 95%, with good sampling effect. The test was carried out using a hand crank actuator for displacement loading, and the fixed end of

the actuator was connected to the load cell and the anchor in turn. During the displacement loading process, 0.25mm was pulled up each time, and the load and displacement were recorded after the sensor was stabilized, after which the next level of displacement was applied.

Table 2. Physical properties of soil samples

Parameters	Unit	
Proportion		2.75
Optimum moisture content	%	23.6
Maximum dry density	g/cm^3	1.63
Dry density	g/cm^3	1.55
Undrained shear strength	kPa	38.6

2.3 Test results

The specimen results and the subsequent MC and HS model simulation results are statistically presented in Table 3. The pullout load-displacement curves under the conditions of L/B=1.4 and H/B=2.4 are plotted as shown in Fig. 1. The analysis shows that the pullout load capacity of anchor plate increases with the increase of burial depth, and the damage displacement (the displacement corresponding to the ultimate load capacity) also increases; at the same time, with the growth of the anchor plate size (the increase of aspect ratio), the pullout load capacity and damage displacement of the anchor plate also increase. The load-displacement curve of the anchor plate pullout process shows a hardening trend, and the load grows with the displacement through three stages successively: 1. Pressure-density growth stage. At this stage, the degree of soil compaction is small, the soil body is constantly compacted, the pullout load increases rapidly with the displacement growth, and the curve shows a certain linearity; 2. Shear damage growth tends to slow down the stage. At this stage, the soil body around the anchor is dense enough, and the soil body around the anchor produces shear damage under the action of anchor plate uplift, forming a rupture surface, and the pullout load decreases. At the same time, the soil above the anchor plate is compacted, causing an increase in the pullout load. This stage of the pullout load with the displacement growth slowed down, until leveling off; 3. Shear residual stage. At this stage, the soil within the influence range of the anchor plate is sufficiently dense, the soil compaction caused by the pullout load growth has been less than the shear damage caused by the pullout load attenuation, the pullout load as a whole with the growth of the uplift displacement and attenuation.

Table 3. Test and finite element simulation results

L/B	H/B	*Q*/kN Test	MC	HS
1(Height 10cm)	2	4.73	6.86	5.32
	4	7.66	9.63	8.53
	6	8.57	11.55	9.88
	8	8.73	12.43	10.26
4(Height 10cm)	2	3.24	4.79	3.77
	4	5.02	7.12	6.16
	6	5.78	8.53	7.34
	8	6.03	9.07	7.83
8(Height 10cm)	2	/	4.45	3.45
	4		6.82	5.68
	6		8.29	6.81
	8		8.76	7.27
strip type(Height 10cm)	2	/	4.23	3.21
	4		6.53	5.32
	6		7.88	6.28
	8		8.28	6.54

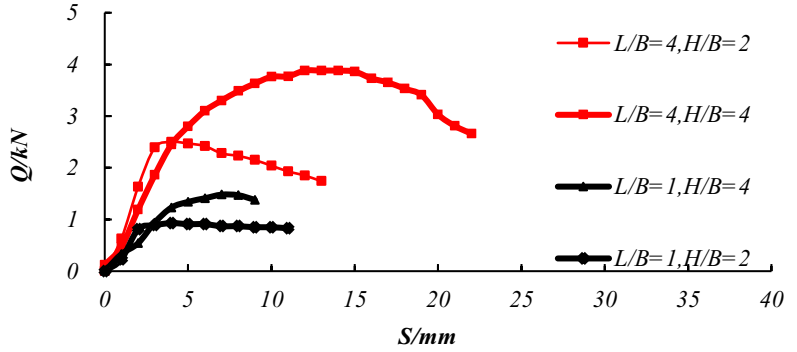

Fig. 1. Pull-out load-displacement curve.

3 Finite element model

3.1 Parameter selection

In order to investigate the internal cause of the geometric effect of the pullout process, a finite element model of the anchor plate pullout test was established based on the model test results to simulate the deformation and damage development process of the uplifted soil body and to determine the ultimate bearing capacity. Plaxis series finite element analysis software was used to calculate the saturated undrained clay (the saturation degree of the soil body under the optimal water content is more than 90%, and the value is taken as saturated for the convenience of calculation) by using the hardened

soil (HS) model based on the Tresca yield criterion and the Moore-Cullen (MC) model. The HS model is a hyperbolic elastic-plastic model put forward by T. Schanz[17] on the basis of the Duncan-Zhang model. hyperbolic elastoplastic model. The model takes into account the shear hardening and compression hardening of the soil, adopts the Moore-Cullen damage criterion, can respond to the stress correlation of the soil stiffness, and is suitable for the description of the deformation and damage characteristics of a variety of soil types[18], which is widely applicable in geotechnical engineering. The HS model contains a total of 11 parameters.

Regarding the values of the HS model parameters, the soil strength parameters were determined with reference to the previously mentioned soil sample characteristic indexes. According to the Plaxis manual[19], m is generally taken as 0.5~1 in clay, and is recommended to be 1. Meanwhile, the manual gives the recommended value of unloading-reloading Poisson's ratio to be 0.2, and the recommended value of the stiffness reference stress to be 100 kPa. the normal consolidation lateral pressure coefficient[20] is taken to be 1. The shear expansion angle, ψ, is taken to be 0 in the case of clays[21]. The HS model parameters selected after analyzing the study are shown in Table 4.

3.2 Modeling and meshing

The computational procedure is performed using small deformation finite element analysis. In order to facilitate the calculation, half of the model is taken for analysis. In the process of mesh establishment, the left, right and lower boundaries of the model are above 10B (plate width) from the axis of the anchor plate, and the rear boundary is above 10L (plate length) from the axis of the anchor plate, which can be considered that the boundary is far enough away from the anchor plate, and it does not affect the pullout bearing of the anchor plate. Mesh division using tetrahedral cells, the anchor week mesh encryption, as shown in Figure 2 for the L/B = 4 finite element model.

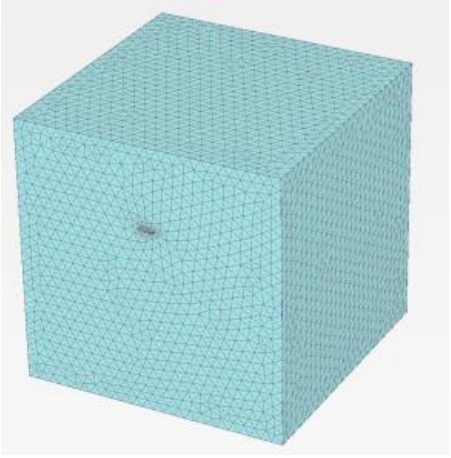

Fig. 2. Finite element model.

Table 4. Finite element simulation parameters

parameters	unit	clay layer	board-shaped
isomorphic model	/	HS	linear elasticity
Type of drainage	/	drainage	non-porous
Υ	kN/m^3	20	80
E_{50}^{ref}	kN/m^2	4000	
E_{oed}^{ref}	kN/m^2	4000	
E_{ur}^{ref}	kN/m^2	20000	
p_{ref}	kN/m^2	100	
S_u	kN/m^2	38.6	
φ'	°	0	/
ψ	°	0	
K_0^{nc}		1	
R_f		0.9	
m	/	1	
v_{ur}		0.2	
v_u		0.495	
E	kN/m^2	/	2*10^8
v	/		0.25

Where: vu is undrained Poisson's ratio and v is anchor plate Poisson's ratio.

3.3 Model validation

In the existing studies[7~10], the analytical comparison process concerning the pullout force of the anchor plate is generally performed by dimensionless processing of the pullout force to obtain the pullout coefficient, and then analyzed by plotting a curve based on the relationship between the ultimate pullout force coefficient and the control variables. The ultimate pullout force of anchor plates in saturated undrained clay is generally expressed as a function of the undrained shear strength:

$$q_u = \frac{Q_u}{A} = S_u N_c \tag{1}$$

Where: Qu indicates the combined force on the anchor plate, qu is the unit area bearing capacity of the anchor plate; A indicates the area of the anchor plate; Su is the undrained shear strength of the soil; Nc is the extreme pullout coefficient of the anchor plate, and it can be seen from the formula that the ultimate pullout coefficient can react to the unit area bearing capacity of the anchor plate.

In Plaxis series software, the interface unit can be set to simulate the contact between anchor plate and soil interface. From the modeling process, it can be seen that under the action of uplift load, the bottom surface of the anchor plate will be quickly detached from the soil body. In order to make the simulation process closer to the actual situation, set the bottom contact surface unit and the soil body for the immediate separation of the loaded form, the interface is set to use the discount method, the discount method

reference[22], according to the experience of the selection of the discount factor Rinter = 0.667. Drawing of the aspect ratio of 1 under the conditions of the HS, MC model calculations of the ultimate coefficient of pullout force - depth of burial ratio curves, and with the results of the model test and the relevant scholarly research results[16,23] for comparison, as shown in Figure 3. The analysis shows that the trend of HS and MC calculation results and model test results are more consistent, and the MC model calculation results are more consistent with the listed research results, and the curves are in between the research results, so it can be considered that the model simulation is reasonable.

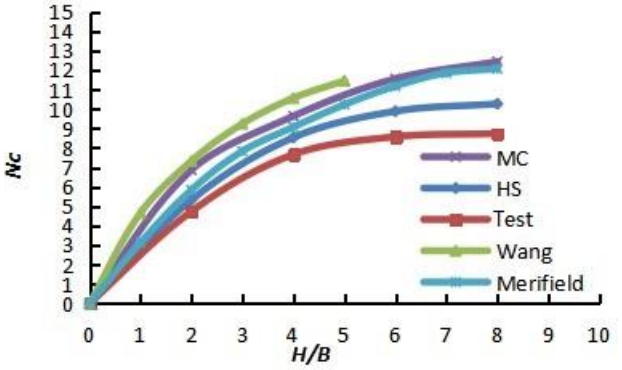

Fig. 3. L/B=1 finite element simulation results.

4 Analysis of numerical results

4.1 A Comparative Study of Models

The curves of ultimate coefficient of pullout force-burial depth ratios obtained from HS and MC model calculations under the conditions of aspect ratios of 1 and 4 are plotted and compared with the curves obtained from the model tests, as shown in Fig. 4.

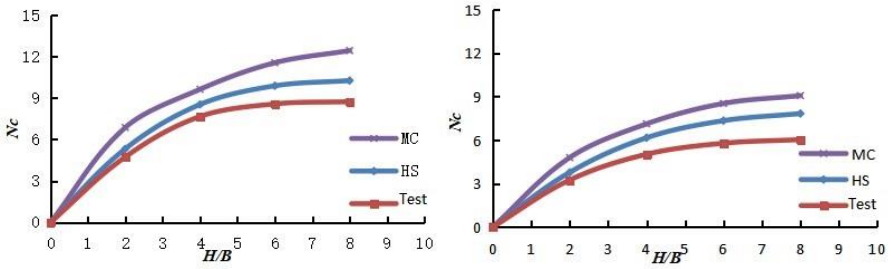

(a)L/B=1 (b)L/B=4

Fig. 4. Comparison of finite element and experimental results.

It can be found that during the pullout process, the ultimate pullout force coefficient of the anchor plate increases gradually with the increase of the burial depth ratio until

it flattens out, and the difference between the simulation results of the MC model and those of the test results is large, with an error of more than 50% at the maximum, which tends to increase with the increase of the burial depth ratio. Compared with the MC model, the HS model is more consistent with the model test results, and the error range of the HS model simulation results is about 11% when H/B<4, which indicates that the HS model can better simulate the pullout process of the anchor plate, so the subsequent analysis is only for the HS simulation results.

As shown in Fig. 5, the ultimate pullout force coefficient-buried depth ratio curves of anchor plates with the same width and different aspect ratios are plotted according to the HS model results. It can be seen that among the anchor plates with rectangular cross-section, the square anchor plate (L/B=1) has the largest ultimate coefficient of pullout resistance, i.e., the square anchor plate has the strongest pullout bearing capacity per unit area compared with other forms. As the aspect ratio increases, the ultimate pullout force coefficient of the anchor plate gradually decreases, and the decay of the ultimate pullout force coefficient of the anchor plate tends to slow down when the aspect ratio is large. From the curve, it can be seen that when L/B=4, the stabilized value of ultimate resistance to pullout coefficient is 7.83, and when L/B=8, the stabilized value of ultimate resistance to pullout coefficient is 7.27, and the relative error between the two is less than 8%, which is a small change. At the same time, it can be seen that the stabilized value of the ultimate load carrying capacity coefficient of the strip anchor plate is 6.54, and the relative error of the ultimate load carrying capacity coefficient when L/B=8 is about 10%, and it can be considered that for the rectangular anchor plate with L/B>8 the load carrying capacity of the pullout is problematic:

$$N_{c_{L/B>8}} \approx N_{c_{\text{stripes}}} \tag{2}$$

Where: indicates L/B=8 rectangular anchor plate ultimate load bearing coefficient, indicates strip anchor plate ultimate load bearing coefficient.

That is, L/B>8 rectangular anchor plate pullout bearing problem is treated as strip anchor plate pullout bearing.

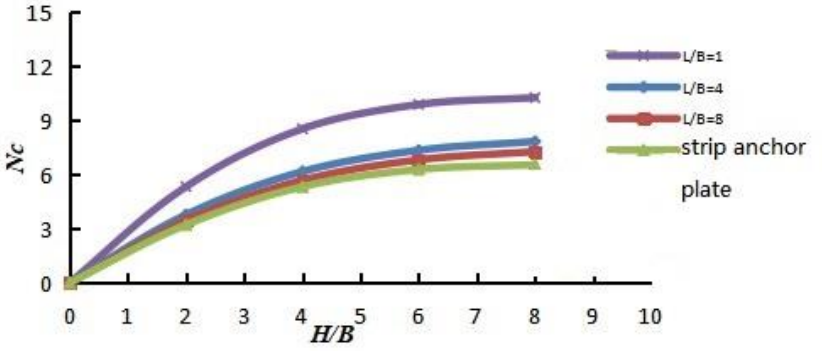

Fig. 5. Comparison of different aspect ratios.

4.2 Characterization of deformation

As shown in Fig.6, the partial strain cloud diagrams of L/B=1 anchor plate and bar anchor plate in the damage state, at H/B=2 and 6 burial depth. Analyzing the graphs, it can be seen that when H/B=2, both kinds of anchor plate deflection strains start from the upper outer edge of the anchor plate outward and upward. Among them, the horizontal inclination of the L/B=1 anchor plate bias strain developing outward is about 46°, while that of the bar anchor plate is about 39°, and the bar anchor plate bias strain is inclined outward to a certain extent.

(a)L/B=1, H/B=2

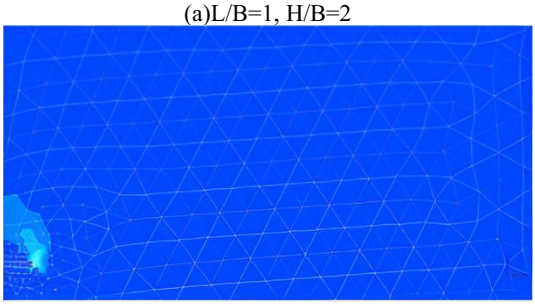

(b)L/B=1, H/B=6

(c)Bar Anchor Plate, H/B=2

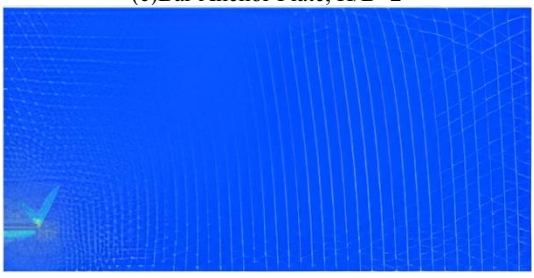

(d)Bar Anchor Plate, H/B=6

Fig. 6. Drawing deviatoric strain cloud diagram.

When H/B=6, the deflection strain of L/B=1 anchor plate gradually develops to the upper part of the anchor plate, forming a closed-loop region inside the soil body, and no deflection strain is generated in the soil body below the closed-loop region, which

is characterized by deep burial; whereas, for the strip anchor plate, the deflection strain appears from the upper side of the anchor plate, and then develops in the direction of the upper part and the outer part of the anchor plate at the same time, which is characterized by both deep burial and shallow burial. The bias strains developed in the direction directly above the anchor plate still form a closed-loop region inside the soil body, and no bias strains are generated in the soil body below the closed-loop region, with the difference that the height of the zero-bias-strain zone is slightly higher. The deviatoric strain developed at the outer side of the anchor plate shows the characteristics of shallow burial, and the deviatoric strain gradually extends to the soil surface with a horizontal inclination angle of about 60°, which is more obvious than the internalization at H/B=2. It can be analyzed that due to the smaller size of L/B=1 anchor plate, compared with the bar anchor plate, the anchor plate is relatively deeper under the same burial depth condition, showing the deep burial characteristics, and the deviatoric strain develops inwardly inclined at H/B=2, whereas the bar anchor plate, due to its relative shallowness, the deviatoric strain has both shallow and deep burial characteristics at H/B=6. The change of the length-to-width ratio of the anchor plate changes the deformation development of the soil around the anchor during the uplift process, and this effect is more significant with the increase of the burial depth.

4.3 Dimensional Impact Analysis

As shown in Fig. 7 is a gray scale diagram of the soil moving shear strength at different displacement state displacements (s is the present displacement and δ is the damage displacement) for H/B=2 and 6 conditions during the pulling process of the bar anchor plate, where the strength curve at a certain point is attached to the H/B=6 diagram.

(a)H/B=2, $s = 0.2\delta$

(b)H/B=2, $s = 0.8\delta$

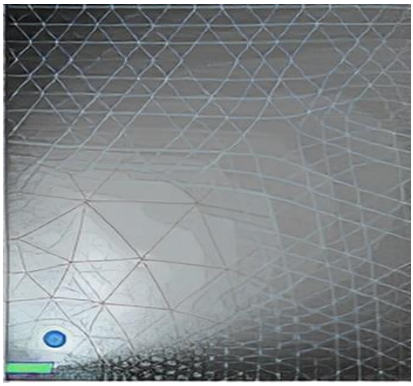

(c)H/B=6, $s = 0.2\delta$

(d)H/B=6, $s = 0.8\delta$

Fig. 7. Moving shear strength nephogram of strip anchor plate.

In Plaxis series software, the moving shear strength distribution can reflect the shear stress state of the soil unit. As shown in Fig. 7(c) and (d), the moving shear strengths of the points at different uplift displacements are shown above the tip box, and the stress state is shown in the following square. Since it belongs to the saturated clay problem (=0), i.e., the damage envelope is perpendicular to the transverse axis, the Moore's dome is the maximum shear stress point suffered by the soil unit, and it can be seen from the figure that the shear stress at this point is equal to the mobile shear strength, so the cloud diagram of the mobile shear strength can reflect the state of the shear stress suffered by the soil body. At the same time, because the HS model adopts Moore-Cullen damage criterion, it can be considered that when the shear stress suffered by the soil body exceeds its shear strength, the soil unit undergoes shear damage.

When the burial depth is shallow (H/B=2), it can be seen from Fig. 7(a) and (b) that the anchor plate pullout process presents shallow burial characteristics: the shear stress on the soil body starts to develop from the upper outer edge of the anchor plate, and extends outward and upward until the soil surface. During this process, the shear stress on the soil body grows gradually until shear damage occurs, and the rupture surface extends gradually upward along the direction of shear stress development;

When the burial depth is deeper (H/B=6), as shown in Fig. 7(c), (d), the anchor plate pullout process presents the transition from shallow burial to deep burial: the shear stress starts to develop from the upper outer edge of the anchor plate, and extends in two directions to the upper part of the anchor plate and the outer part of the plate. The shear stress in a certain range of soil below the shear zone above the anchor plate is 0, forming a triangular core area, and the shear stress at the junction of the core area and the shear zone is more concentrated, and the soil layer rupture is obvious. At the same time, with the increase of uplift displacement, the shear stress develops outside the plate, forming a rupture zone with outward tension. Throughout the process, the soil shear stress undergoes a gradual growth process until the rupture surface is formed. In addition, the gradual growth process is more significant in the deeply buried condition compared to the shallow buried condition.

As shown in Figs. 8, 9 and 10, the gray scale diagrams of the soil mobile shear strength for different displacement states of L/B=1,4,8 anchor plates for H/B=2 and 6 conditions. Comparing the images at H/B=2, it can be seen that the anchor plate pullout process shows shallow burial characteristics: with the increase of the anchor plate aspect ratio L/B, the anchor plate shear stress extends outward up to the soil surface. At the same time, the outward inclination angle of the rupture surface increases with the growth of the aspect ratio, and the shallow burial characteristic of anchor plate with large aspect ratio is more significant. It can be analyzed that when the rectangular anchor plate has the same width, with the growth of the anchor plate aspect ratio, the anchor plate area is larger, and under the same burial depth ratio H/B, the large anchor plate is shallower than the small anchor plate, which shows more obvious shallow burial characteristics.

Comparing the image when H/B=6, it can be seen that, firstly, with the increase of anchor plate burial depth, the soil unit shear stress is changed from expanding outward to expanding to the upper part of the anchor plate, and a circular shear zone is formed in the inner part of the anchorage plate when it reaches a specific depth, which has a deep burial characteristic. At the same time, the shear zone below the formation of obvious triangular core area, the core area is not subject to shear stress, the core area and the shear zone at the interface of the shear stress distribution is concentrated, the soil rupture is significant. Secondly, with the growth of anchor plate aspect ratio, it can be clearly observed that the soil pullout damage process around the plate is gradually changed from deeply buried to shallowly buried. L/B=1 anchor plate pullout process in the soil body to form a circular shear zone, resulting in a circular rupture surface, for the deeply buried characteristics. And the rest of the anchor plate pulling process appears to the outside of the plate upward development of the shear zone, the formation of the external tension rupture surface, for the deep burial to shallow burial transition characteristics. And the larger L/B is, the more obvious the extensional process is. In the process of research, the depth ratio of anchor plate at the limit of shallow and deep burial is usually defined as the critical depth ratio (H/B) cr. From the characteristics of the anchor plate drawing process, it can be seen that, for L/B=1 anchor plate, the anchor plate is already in deep burial state when H/B=6, and the critical depth ratio (H/B) $Cr \leq 6$, while for L/B=4 and 8 anchor plate, the anchor plate has not yet reached the deep burial state when H/B=6, and the critical depth ratio (H/B) $Cr \geq 6$, i.e., the length-to-width ratio

of the anchor plate is more than 6.1 mm, which means that the anchor plate has the same length and width ratio as the anchor plate, but with a larger width ratio of the anchor plate. , i.e., the growth of the anchor plate aspect ratio makes (H/B) Cr increase. In addition, the progressive damage process of the soil body is more significant under deep burial condition, and the change of shear stress distribution is more obvious.

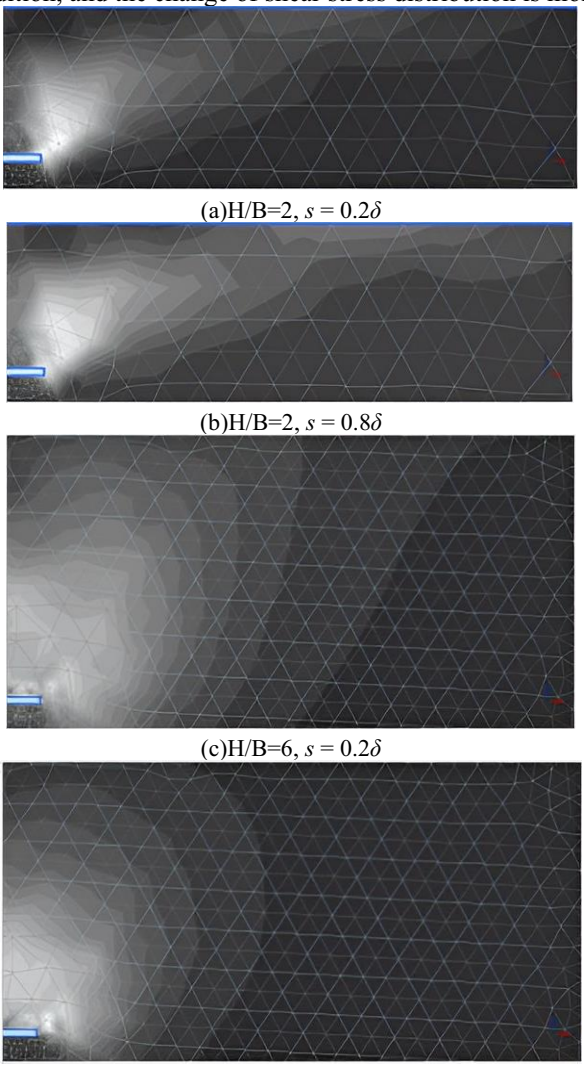

(a)H/B=2, $s = 0.2\delta$

(b)H/B=2, $s = 0.8\delta$

(c)H/B=6, $s = 0.2\delta$

(d)H/B=6, $s = 0.8\delta$

Fig. 8. L/B=1 anchor plate moving shear strength nephogram.

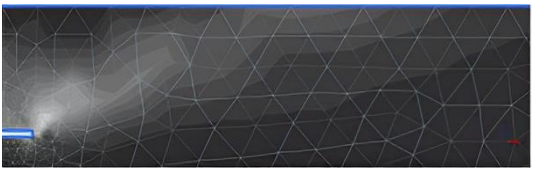

(a)H/B=2, $s = 0.2\delta$

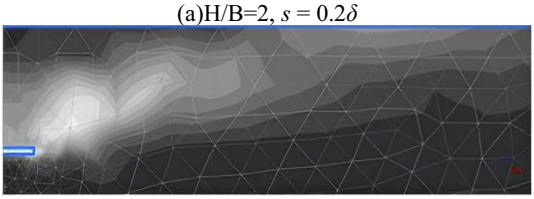

(b)H/B=2, $s = 0.8\delta$

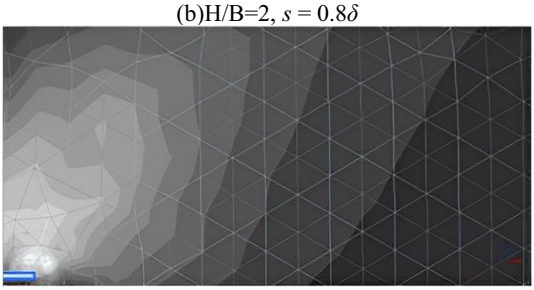

(c)H/B=6, $s = 0.2\delta$

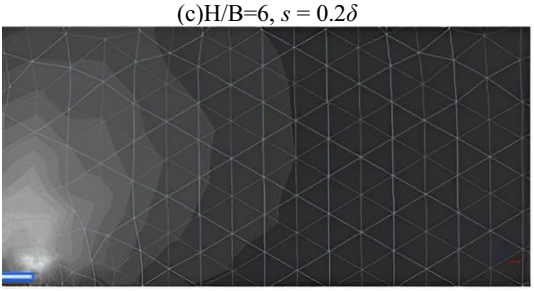

(d)H/B=6, $s = 0.8\delta$

Fig. 9. L/B=4 anchor plate moving shear strength nephogram.

(a)H/B=2, $s = 0.2\delta$

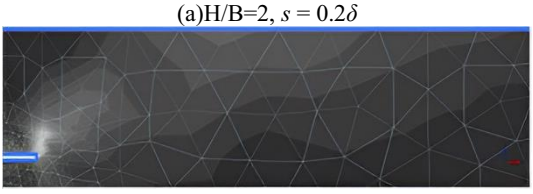

(b)H/B=2, $s = 0.8\delta$

(c)H/B=6, $s = 0.2\delta$

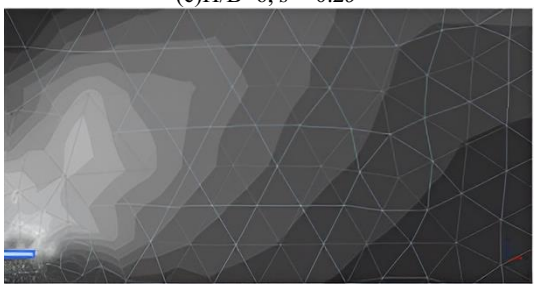

(d)H/B=6, $s = 0.8\delta$

Fig. 10. L/B=8 anchor plate moving shear strength nephogram.

5 Conclusion

Through the indoor model test and finite element analysis method, the research on the effect of rectangular anchor plate geometry on the anchorage bearing characteristics in clay soil was carried out, and the effect of the long side of the anchor plate on the uplift bearing capacity and the damage morphology of the soil around the anchor and the reasons for it were analyzed, and the conclusions were obtained as follows:

(1) Anchor plate pulling process load-displacement curve shows a hardening trend, load with the displacement growth has experienced three stages: pulling the early stage, the upward pulling process makes the soil body continue to compact, the rapid increase in the pullout load, and upward pulling displacement presents a certain linearity for the compacting growth stage; a certain upward pulling displacement, the soil body around the anchor has been sufficiently dense, the upward pulling process continues to make the soil body shear damage, resulting in pullout After a certain upward displacement, the soil around the anchor is sufficiently dense, and the upward pulling process continues to make the soil shear damage, resulting in a certain attenuation of the pullout load, and the growth of the pullout load gradually slows down until flattening, which is the stage of slowing down of the growth of the shear damage. At the same time, it can be observed that the ultimate pullout load of the anchor plate increases with the increase of the depth of burial or the area of the anchor plate, and the pullout bearing capacity of the anchor plate is increasing. However, with the growth of the anchor plate area (increase in aspect ratio), the anchor plate unit area bearing capacity decreases, and the size of the anchor plate has an effect on the anchor plate pullout bearing.

(2) The uplift damage process of the anchor plate starts from the outer edge of the upper side of the plate first, showing a gradual damage pattern. The soil at the upper outer edge of the plate is first damaged by shear, and the shear stress beyond its shear strength will continue to spread to the surrounding soil, causing further damage to the surrounding soil. When the anchor plate is shallowly buried (corresponding to H/B=2), a rupture surface from the upper edge of the plate outward and upward to the soil surface is eventually generated. When the anchor plate is deeply buried (H/B≥6), a ring-shaped rupture surface is formed inside the soil directly above the anchor plate, and a triangular shear-free zone is formed in a certain area below the rupture surface, and the height of the triangular shear-free zone is affected by the depth of burial and the size of the anchor plate.

(3) Differences in the aspect ratio of the anchor plate change the development process of uplift progressive damage, which has a significant effect on the anchor plate anchorage bearing characteristics. The same width anchor plate, with the growth of the aspect ratio, the critical depth of burial ratio increases. At the same depth of burial, the shear stress-strain development of the soil body around the anchor during the pullout process is more obvious, more shallow burial characteristics, resulting in different anchor plate anchorage bearing capacity.

Acknowledgments

This work was financially supported by the National Natural Science Foundation of China (No.51709016), the basic scientific research business fees of central public welfare research institutes.

(No.CKSF2019199 / YT), and the umbrella anchor demonstration project (SF-202201) of the water conservancy technology development project plan of the Ministry of Water Resources.

References

1. Cheng Yonghui, Wang Manxing, Xiong Yong. Application of Umbrella Anchor in Temporary Slope Reinforcement of Expansive Soil in North Hubei Water Diversion Project [J]. Journal of Yangtze River Academy of Sciences, 2019, 36 (04): 71-76.
2. Cheng Zhanlin, Cheng Yonghui, Guo Xiling and so on. A special impact umbrella anchor for emergency rescue: China, ZL201520512552.0 [P].2016-01-20.
3. Qian Pingyi, Liu Zude, Liu Yiliang. Deformation and failure characteristics of soil around shallow inclined anchor plate [J]. Journal of Geotechnical Engineering, 1992 (01) : 62-66.
4. Gao Yuxin, Zhu Honghu, Zhang Chunxin, Liu Wei, Wang Jing, Zhang Wei. Simulation of anchor plate uplift in sand by three-dimensional material point method [J]. Chinese Journal of Geotechnical Engineering, 2022, 44 (02): 295-304.
5. Hu Wei, Meng Jianwei, Yao Chen, Lei Yong. Calculation method of vertical pull-out ultimate bearing capacity of shallow-buried flat circular anchor [J]. Geotechnical Mechanics, 2020,41 (09) : 3049-3055.DOI : 10.16285 / j.rsm. 2019. 2070.
6. White. D.J, Cheuk. C.Y, Bolton. M.D. The uplift resistance of pipes and plate anchors buried in sand[J]. Géotechnique, 2008, 58(10):771–779.

7. Su Fangmei, Liu Haixiao, Li Zhou. Numerical analysis of the ultimate bearing capacity of anchor plates in clay based on the coupled Euler-Lagrangian method [J]. Geotechnical mechanics, 2016,37 (09) : 2728-2736.DOI: 10.16285 / j.rsm.2016.09.039.
8. Yu Long, Liu Jun, Kong Xianjing. Bearing capacity of anchor plate in normally consolidated clay [J]. Geomechanics, 2007 (07): 1427-1434.DOI: 10.16285 / j. rsm. 2007. 07.027.
9. Wang Lizhong, Shu Heng. Pullout capacity of deep-buried anchor plates in undrained clay [J]. Journal of Geotechnical Engineering, 2009,31 (06) : 829-836.
10. Yu Shengbing, Huang Maosong. Uplift capacity analysis of strip anchor plate based on upper bound method [J]. Geotechnical mechanics,2010,31(S2):160-163. DOI: 10. 16285/ j.rsm. 2010. s2.064.
11. Hao Dongxue, Fu Shengnan, Chen Rong, Zhang Yongjian, Hou Liqun. Pull-out model test and pull-out force calculation of anchor plate in sand [J]. Journal of Geotechnical Engineering, 2015,37 (11 : 2101-2106.
12. Chen Rong, Fu Shengnan, Hao Dongxue, Shi Danda. Size effect analysis of uplift bearing capacity of circular anchor in dense sand [J]. Chinese Journal of Geotechnical Engineering, 2019,41 (01): 78-85.
13. Shi Danda, Mao Yiyao, Yang Yong, Yuan Yuan, Hao Dongxue. Experimental study on deformation characteristics of uplift soil of circular anchor plate in sand based on DIC technique [J]. Geotechnical mechanics,2020,41(10):3201-3213. DOI:10.16285 / j.rsm. 2020.0096.
14. Das, B.M., 1978. Model tests for uplift capacity of foundations in clay. Soils and Foundations,18(2):17-24.
15. Rowe. R.K, Davis. E.H. The behaviour of anchor plates in clay[J].Géotechnique,1982,32(1):9-23.DOI:10.1680/geot.1982.32.1.9.
16. Wang Dong, Hu Yuxia, Randolph Mark F. Three-Dimensional Large Deformation Finite-Element Analysis of Plate Anchors in Uniform Clay[J]. Journal of Geotechnical and Geoenvironmental Engineering. 2010,136, (2):355-365.
17. SCHANZ T, VERMEER P A, BONNIER P G. The Hardening Soil model: formulation and verification[C]// Beyond 2000 in Computational Geotechnics—10 years of PLAXIS. Amsterdam: [s. n.], 1999: 281-296.
18. BRINKGREVE R B J. Selection of soil models and parameters for geotechnical engineering application[C]// Proceedings of Geo-Frontier Conference. Texas: Soil Properties and Modeling Geo-Institute of ASCE, 2005: 69-98.
19. BRINKGREVE R B J, BROERE W. Plaxis material models manual[M]. Delft: [s. n.], 2006.
20. GAO D Z, WEI D D, HU Z X. Geotechnical properties of Shanghai soils and engineering applications[M]// CHANEY RONALD C. Marine Geotechnology and Nearshore/offshore Structures. Philadelphia: ASTM, 1986: 161-178.
21. JANBU J. Soil compressibility as determined by oedometer and triaxial tests[C]//Proceedings of the 3rd European Conference on Soil Mechanics and Foundation Engineering. Wiesbaden: [s.n.], 1963.
22. Zuo Jianzhong, Jiang Xin, Fu Yongguo, Chen Xinni, Huang Cenyi, Qiu Yanjun. Numerical simulation of embankment reinforcement based on PLAXIS and OPTUM [J].Traffic Science and Technology, 2022 (01) : 5-10.
23. MERIFIELD R S, SLOAN S W, YU H S. Stability of plate anchors in undrained clay[J]. Geotechnique, 2001, 51(2): 141-153.